Evaluation of Lung Cancer and Neuroendocrine Neoplasm in a Single Scan by Targeting Both Somatostatin Receptor and Integrin $\alpha_v\beta_3$

Yumin Zheng, MD,† Hanping Wang, MD,‡ Huangying Tan, MD,§ Xiaoxia Cui, MD,‡ Shaobo Yao, PhD,*|| Jie Zang, MD,* Li Zhang, MD,‡ and Zhaohui Zhu, MD¶*

Abstract: Purpose: This pilot study aimed to prove the complementary value of a novel ^{68}Gallium-labeled heterodimeric peptide, ^{68}Ga-NOTA-3P-TATE-RGD, in detection and evaluation of tumors with somatostatin receptor subtype 2 or integrin $\alpha_v\beta_3$ overexpression, including non-small cell lung cancer (NSCLC), small-cell lung cancer (SCLC), neuroendocrine tumor (NET), and neuroendocrine carcinoma (NEC).

Methods: With institute review board approval and written informed consent, 32 patients with pathologically diagnosed lung cancer (18 NSCLC, 14 SCLC) and 12 patients with neuroendocrine neoplasm (8 NET, 4 NEC) patients were recruited to undergo ^{68}Ga-NOTA-3P-TATE-RGD PET/CT. For comparison, the NSCLC patients also underwent ^{68}Ga-NOTA-TATE PET/CT, the SCLC patients underwent ^{68}Ga-NOTA-RGD PET/CT, and the neuroendocrine neoplasm patients underwent ^{18}F-FDG PET/CT within 3 days. The maximum standardized uptake value (SUV) of the primary tumor (T) and mean SUV of the blood pool (B) were measured, and the T/B ratios were calculated for comparison.

Results: In the primary tumors of NSCLC, the T/B ratios of ^{68}Ga-NOTA-3P-TATE-RGD were significantly higher than those of ^{68}Ga-NOTA-TATE (4.54 ± 3.00 versus 4.10 ± 2.83, $P = 0.0058$). In SCLC, the T/B ratios of ^{68}Ga-NOTA-3P-TATE-RGD were significantly higher than those of ^{68}Ga-NOTA-RGD (6.06 ± 6.09 versus 2.65 ± 1.19, $P = 0.0344$). In NET, the T/B ratios of ^{68}Ga-NOTA-3P-TATE-RGD were 36.13 ± 33.84, significantly higher than those of ^{18}F-FDG (2.91 ± 1.71, $P = 0.0234$). In NEC, there were no significant difference between the T/B ratios of ^{68}Ga-NOTA-3P-TATE-RGD (4.80 ± 0.85) and those of ^{18}F-FDG (3.56 ± 0.74, $P = 0.1833$).

Conclusions: This proof-of-concept study preliminarily demonstrates the efficacy of the dual targeting ^{68}Ga-NOTA-3P-TATE-RGD PET/CT in the evaluation of lung cancer and neuroendocrine neoplasm in a single scan.

Key Words: positron emission tomography, integrin $\alpha_v\beta_3$, somatostatin receptor, ^{68}Ga-NOTA-3P-TATE-RGD, lung cancer, neuroendocrine neoplasm

(*Clin Nucl Med* 2019;44: 687–694)

Over the past decade, radiolabeled receptor-targeted peptides have been extensively investigated because of their potential use as both imaging probes and therapy agents to target a wide range of tumors.[1,2] Many peptide-based radiotracers have been explored and have shown promising results in experimental studies, and some have been successfully translated into clinical use.[3]

Radiolabeled octreotide analogs, such as ^{111}In-octreotide, ^{99m}Tc-HYNIC-TOC, and ^{68}Ga-DOTATATE, specifically target somatostatin receptors (SSTRs), high-affinity G protein-coupled membrane receptors expressed in neuroendocrine cells, and other cell types.[4] SSTR imaging has been found useful not only for the diagnosis of neuroendocrine neoplasm (NEN)[5] but also for evaluation of lung cancer, especially for small cell lung cancer (SCLC) overexpressing SSTR subtype 2 (SSTR2).[6,7] ^{68}Ga-DOTATATE is one of the promising peptides with high affinity to SSTR2; however, it has relatively low uptake in non-small cell lung cancer (NSCLC).[8]

Arg-Gly-Asp (RGD) peptide-based radiotracers have been developed for imaging of integrin $\alpha_v\beta_3$ overexpression in various tumor types.[9–11] Clinical investigations of radiolabeled RGD peptides for noninvasive visualization of tumor integrin expression have demonstrated their efficacy in the diagnosis and staging of a variety of common malignancies in humans, including lung cancer, glioma, breast cancer, and head-and-neck carcinoma.[12–16] Moreover, ^{68}Ga-NOTA-PRGD2 PET/CT imaging is found more specific than ^{18}F-FDG PET/CT in the assessment of lymph node metastasis of lung cancer.[15] However, because of the lower integrin $\alpha_v\beta_3$ expression in small-cell lung cancer, the uptake of ^{68}Ga-RGD2 in SCLC is significantly lower than that in NSCLC.[16]

In this study, we conjugated 2 monomeric peptides, TATE and RGD, with the macrocyclic chelator 1,4,7-triazacyclononane-N, N′,N″-triacetic acid (NOTA), using 3 polyethylene glycol $(PEG)_4$ as linked spacers; then, the heterodimeric peptide NOTA-3P-TATE-RGD was labeled with ^{68}Ga. The scientific hypothesis was that the novel PET tracer can accumulate in tumors with overexpression of either SSTR2 or integrin αvβ3. ^{68}Ga-NOTA-3P-TATE-RGD was designed to compare with each monomeric radiotracer, ^{68}Ga-NOTA-TATE and ^{68}Ga-NOTA-RGD, in the evaluation of NSCLC and SCLC, respectively, to prove the complementary value of the dual-targeting tracer, especially in making up for the insufficiency of the TATE imaging in NSCLC and the RGD imaging in SCLC. In addition, ^{68}Ga-NOTA-3P-TATE-RGD was preliminarily compared with ^{18}F-FDG, the most commonly used PET tracer, in the evaluation of patients with neuroendocrine tumor (NET) or neuroendocrine cancer (NEC), so as to further clarify the extended value of the dual target imaging tracer.

Received for publication November 12, 2018; revision accepted May 9, 2019.
From the *Department of Nuclear Medicine and Beijing Key Laboratory of Molecular Targeted Diagnosis and Therapy in Nuclear Medicine, Peking Union Medical College (PUMC) Hospital, Chinese Academy of Medical Sciences (CAMS) and PUMC; †Department of Nuclear Medicine, China-Japan Friendship Hospital; ‡Respiratory Department, PUMC Hospital, CAMS and PUMC; §Department of Integrative Oncology, China-Japan Friendship Hospital, Beijing; ||PET-CT Center, General Hospital of Tianjin Medical University, Tianjin; and ¶Key Laboratory of Endocrinology of National Health and Family Planning Commission, PUMC Hospital, CAMS and PUMC, Beijing, People's Republic of China.
Conflicts of interest and sources of funding: This study was partly supported by the Key Special Project on Inter-Governmental Scientific and Technological Innovation Cooperation in National Key Research and Development Plan (2016YFE0115400), the Chinese Academy of Medical Science Major Collaborative Innovation Project (2016-I2M-1-011), National Nature Science Foundation (81741142, 81871392), and Beijing Municipal Natural Science Foundation (7161012). None declared to all authors.
Correspondence to: Zhaohui Zhu, MD, Department of Nuclear Medicine, Peking Union Medical College (PUMC) Hospital, Chinese Academy of Medical Sciences and PUMC, Beijing 100730, People's Republic of China. E-mail: zhuzhh@pumch.cn.

ISSN: 0363-9762/19/4409–0687
DOI: 10.1097/RLU.0000000000002680

PATIENTS AND METHODS

Patient Enrolment

This clinical trial was approved by the institutional review board of Peking Union Medical College Hospital, Chinese Academy of Medical Sciences, and Peking Union Medical College. It was registered in ClinicalTrials.gov (NCT02817945). All recruited subjects provided written informed consent.

A total of 32 biopsy-diagnosed lung cancer patients (age range, 36–79 years; mean, 59 ± 12 years), including 18 patients with NSCLC and 14 patients with SCLC, were enrolled to undergo ^{68}Ga-NOTA-3P-TATE-RGD PET/CT. The inclusion criteria were age 18 to 80 years, presence of a solid lung nodule or mass with a diameter greater than 2 cm, tumor identification by bronchoscope- or CT-guided biopsy as NSCLC or SCLC, and patient's readiness to provide clinical information and follow-up. The exclusion criteria included claustrophobia, kidney or liver failure, and inability to complete the study. The demographic characteristics of the patients are shown in Table 1. Among the patients, 18 NSCLC patients also underwent ^{68}Ga-NOTA-TATE PET/CT, and 14 SCLC patients underwent ^{68}Ga-NOTA-RGD PET/CT within 3 days for comparison.

In addition, 12 patients (age range, 39–63 years; mean, 50 ± 7 years) with NEN, including 8 NET and 4 NEC, were recruited to undergo ^{68}Ga-NOTA-3P-TATE-RGD PET/CT. Among the 8 NET patients, one was in WHO grade 1 (G1, Ki67 < 1%), 5 in G2 (Ki67 from 3% to 10%), and one in G3 (Ki67 25%). The 4 NEC were originated from gastroenteropancreatic regions with Ki67 from 50% to 70%. All NEN patients had multiple liver and/or lymph node metastasis. They all underwent ^{18}F-FDG PET/CT within 3 days for comparison.

Radiopharmaceutical Preparation

NOTA-3P-TATE-RGD were conjugated by binding the monomeric TATE and RGD with the macrocyclic chelator NOTA through 3 PEG_4 as linked spacers. The chemical structure (Fig. 1) was designed by the authors and synthesized by CS Biotechnology Company (Menlo Park, CA). NOTA-TATE and NOTA-RGD were also obtained through the same route for comparison.

^{68}Ga labeling of NOTA-3P-TATE-RGD, NOTA-TATE, or NOTA-RGD was prepared using the methods described previously.[15] Briefly, ^{68}Ga was eluted from a ^{68}Ge/^{68}Ga generator (ITG, Berlin, Germany) using 0.1 M hydrochloric acid (HCl) and mixed with 1.25 M sodium acetate (NaOAc) buffer solution to achieve a pH of 4.0. Then, 30 to 50 μg NOTA-3P-TATE-RGD (or NOTA-TATE, or NOTA-RGD) dissolved in pure water was added to the vial of mixture. The reaction was carried out at 100°C for 10 minutes. The radiochemical purity of ^{68}Ga-NOTA-3P-TATE-RGD (or ^{68}Ga-NOTA-TATE or ^{68}Ga-NOTA-RGD) was determined by thin layer chromatography (BioScan, Washington DC, USA), using CH3OH: NH4OAc (v/v 1:1) as the developing solution. If exceeded 95%, the product was passed through a 0.22-μm filter directly into a sterile vial for patient injection.

PET/CT Scanning and Image Analysis

For the patients, the synthesized ^{68}Ga-NOTA-3P-TATE-RGD (or ^{68}Ga-NOTA-TATE or ^{68}Ga-NOTA-RGD) was injected intravenously at a dose of approximately 1.85 MBq (0.05 mCi) per kilogram of body weight. For ^{18}F-FDG PET/CT scanning, the patients fasted for at least 4 hours, and their blood glucose levels measured less than 6.4 mmol/L before intravenous injection of ^{18}F-FDG in a dosage of approximately 5.55 MBq (0.15 mCi) per kilogram of body weight.

TABLE 1. Patients' Demographic Information, Histological Diagnosis, and Semiquantitative Imaging Values

	Lung Cancer			Neuroendocrine Neoplasm	
	^{68}Ga-TATE-RGD	^{68}Ga-TATE	^{68}Ga-RGD	^{68}Ga-TATE-RGD	^{18}F-FDG
Age (yr)					
Range	36–79	44–79	36–79	39–63	39–63
Mean ± SD	59 ± 12	57 ± 12	61 ± 11	50 ± 7	50 ± 7
Sex					
Male	17	9	8	5	5
Female	15	9	6	7	7
Pathology					
	SCLC: 14		SCLC: 14	NET: 8	NET: 8
	NSCLC: 18	NSCLC: 18		G1: 1 (Ki67 < 1%)	G1: 1
	AC: 15	AC: 15		G2: 5 (Ki67 3%-10%)	G2: 5
	ASC: 2	ASC: 2		G3: 1 (Ki67 25%)	G3: 1
	SCC: 1	SCC: 1		NEC: 4 (Ki67 50%-70%)	NEC: 4
SUVmax	4.07 ± 4.00				
	4.99 ± 5.25 (SCLC: 14)		2.08 ± 0.97, (P = 0.0401)	24.12 ± 22.39 (NET: 8)	3.75 ± 2.81 (P = 0.0241)
	3.35 ± 2.61 (NSCLC: 18)	2.87 ± 2.15 (P = 0.0050)		4.89 ± 0.87 (NEC: 4)	5.10 ± 1.07 (P = 0.8282)
T/B ratio	5.21 ± 4.59				
	6.06 ± 6.09 (SCLC: 14)		2.65 ± 1.19, (P = 0.0344)	36.13 ± 33.84 (NET: 8)	2.91 ± 1.71 (P = 0.0234)
	4.54 ± 3.00 (NSCLC: 18)	4.10 ± 2.83, (P = 0.0058)		4.80 ± 0.85 (NEC: 4)	3.56 ± 0.74 (P = 0.8282)

SCLC indicates small cell lung cancer; NSCLC, non-small cell lung cancer; AC, adenocarcinoma; ASC, adenosquamous carcinoma; SCC, squamous cell carcinoma; NET, neuroendocrine tumor; NEC, neuroendocrine cancer; SUVmax, maximum standardized uptake value; T/B ratio, the tumor to blood pool radioactivity ratio.

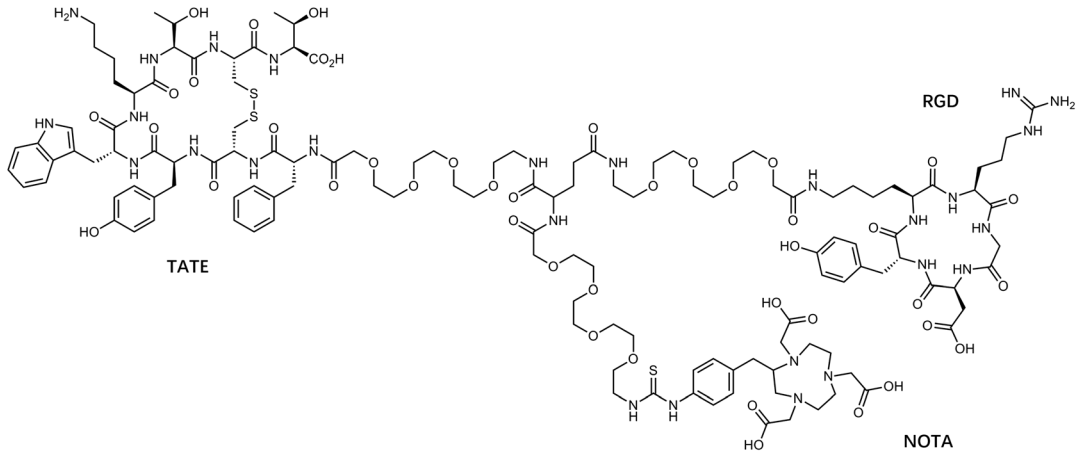

FIGURE 1. Chemical structure of NOTA-3P-TATE-RGD heterodimer. The monomeric TATE and RGD, and the macrocyclic chelator 1,4,7-triazacyclononane-N,N′,N″- triacetic acid (NOTA), were linked with 3 polyethylene glycol $(PEG)_4$ spacers.

PET/CT imaging was performed 40 to 60 minutes after tracer administration using a Biograph 64 True V system (Siemens Medical Solutions, Knoxville, TN). After a low-dose CT imaging (120 kV, 35 mA, 3-mm layer, 512 × 512 matrix, 70 cm FOV), whole-body PET imaging was performed from the upper thigh to the skull bottom (2 minutes per bed position, 5 to 6 bed positions depending on the height of a patient). The emission data were corrected for randoms, dead time, scattering, and attenuation. Ordered subsets expectation maximum reconstruction algorithm was used, and the images were zoomed with a factor of 1.2.

The images were then transferred to a MMWP workstation (Siemens Medical Solutions) for visual and semiquantitative analysis by 2 experienced nuclear medicine physicians. They reached a consensus if there was a discrepancy. The volume of interest of a normal organ/tissue and concerned lesion was drawn over the images using a 3D isocontour method with the assistance of corresponding CT images by the same experienced nuclear medicine physician. Standardized uptake values (SUVs) in the volumes of interest were obtained through the software. The maximum SUV (SUVmax) of the tumor (T), specifically the primary tumor of lung cancer and the main tumor of NEN, were measured. The mean SUV (SUVmean) of blood pool (B) and other normal organs were also obtained. T/B ratios were calculated by dividing the T and B values.

Pathological Analysis and Immunohistochemical Staining

The pathological diagnosis was determined by 2 experienced pathologists independently, and they reached consensus by referring to a third pathologist when there was any discrepancy.

For immunohistochemical staining, representative tumor tissue sections were fixed with 10% neutral buffered formalin and embedded in paraffin. After blocking and washing, 5-μm-thick tissue sections were incubated with mouse antihuman monoclonal antibody against human SSTR2A (PA3–109, Thermo Fisher Scientific) and integrin $\alpha_v\beta_3$ (ab78289, Abcam). Six fields were randomly selected from each section and observed using a light microscope (BX41, Olympus). For semiquantification of SSTR2A and integrin $\alpha_v\beta_3$ expression, 5 entire high-power fields (×40) containing clusters of malignant cells were identified randomly per slide and scored for intensity and percentage of SSTR2A and integrin $\alpha_v\beta_3$ staining expression.

Statistical Analysis

The quantitative data are expressed as means ± standard deviations. Differences in radiotracer uptake between 2 independent groups were determined using the Student *t* tests. Paired *t* test was used to compare the difference in tracer uptake in the same patients. A threshold of $P < 0.05$ was considered significant. All statistical analysis was performed using SPSS 23.0 software (IBM SPSS, Chicago, IL).

RESULTS

In the 32 lung cancer patients and the 12 NEN patients who underwent ^{68}Ga-NOTA-3P-TATE-RGD PET/CT, no remarkable adverse effect was observed that correlated with the tracer injection. The quality of the images was read as good in all patients. The background uptake of ^{68}Ga-NOTA-3P-TATE-RGD was quite low in the lungs, blood pool, muscles, and bone marrow, with similar low level of SUVmean as those of ^{68}Ga-NOTA-TATE and ^{68}Ga-NOTA-RGD (Fig. 2). ^{68}Ga-NOTA-3P-TATE-RGD was excreted mainly through the kidneys. Without coinfused cationic amino acids to inhibit renal tubular reabsorption in these patients, the renal uptake level of ^{68}Ga-NOTA-3P-TATE-RGD reached a level of SUVmean 23.09 ± 5.93, almost 3 fold of the ^{68}Ga-NOTA-TATE uptake and 5 fold of the ^{68}Ga-NOTA-RGD uptake (Fig. 2). The spleen showed a lesser intense ^{68}Ga-NOTA-3P-TATE-RGD uptake (SUVmean = 13.02 ± 2.90), which was lower than the ^{68}Ga-NOTA-TATE uptake but remarkably higher than the ^{68}Ga-NOTA-RGD uptake. The liver uptake of ^{68}Ga-TATE-RGD (SUVmean = 1.94 ± 0.40) was mild, significantly lower than that of ^{68}Ga-NOTA-TATE but mildly higher than that of ^{68}Ga-NOTA-RGD. ^{68}Ga-NOTA-3P-TATE-RGD uptake was observed in all known primary lung tumors with high contrast. The SUVmax ranged from 0.85 to 18.21 (4.07 ± 4.00), and the T/B ratios were from 1.25 to 20.23 (5.21 ± 4.59). There was no significant difference between the SUVmax of SCLC (4.99 ± 5.25, n = 14) and that of NSCLC (3.35 ± 2.61, n = 18; $P = 0.257$), and between the T/B ratio of SCLC (6.06 ± 6.09) and that of NSCLC (4.54 ± 3.00; $P = 0.3625$) as well.

In the 18 patients with NSCLC who underwent both ^{68}Ga-NOTA-3P-TATE-RGD and ^{68}Ga-NOTA-TATE PET/CT within 3 days, the SUVmax of ^{68}Ga-NOTA-3P-TATE-RGD (3.35 ± 2.61) was significantly higher than that of ^{68}Ga-NOTA-TATE (2.87 ± 2.15, $P = 0.005$) (Fig. 3); the T/B ratio of ^{68}Ga-NOTA-3P-TATE-RGD (4.54 ± 3.00) was significantly higher than that of ^{68}Ga-NOTA-TATE (4.10 ± 2.83,

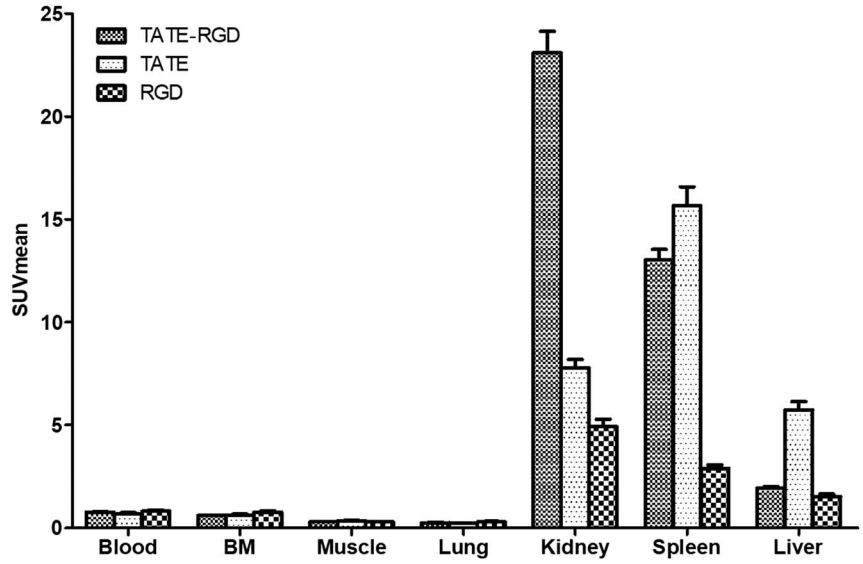

FIGURE 2. The SUVmean of the blood pool and some normal tissues on ^{68}Ga-NOTA-3P-TATE-RGD, ^{68}Ga-NOTA-TATE, and ^{68}Ga-NOTA-RGD PET/CT imaging. The blood pool, muscles, bone marrow (BM), and lung showed quite low uptake. ^{68}Ga-NOTA-3P-TATE-RGD was mainly excreted through the kidneys; the spleen showed intense physiological uptake similar to the pattern of ^{68}Ga-NOTA-TATE, and the liver showed relatively lower uptake similar to the pattern of ^{68}Ga-NOTA-RGD.

P = 0.0058) (Fig. 3). Among these patients with NSCLC, integrin $\alpha_v\beta_3$ staining showed strong positivity, and SSTR2A staining revealed moderate positivity (Fig. 4).

In the 14 patients with SCLC who underwent both ^{68}Ga-NOTA-3P-TATE-RGD and ^{68}Ga-NOTA-RGD PET/CT within 3 days, the SUVmax of ^{68}Ga-NOTA-3P-TATE-RGD (4.99 ± 5.25) was significantly higher than that of ^{68}Ga-NOTA-RGD (2.08 ± 0.97, P = 0.0401) (Fig. 3); the T/B ratio of ^{68}Ga-NOTA-3P-TATE-RGD (6.06 ± 6.09) was significantly higher than that of ^{68}Ga-NOTA-RGD (2.65 ± 1.19, P = 0.0344) (Fig. 3). SSTR2A staining showed

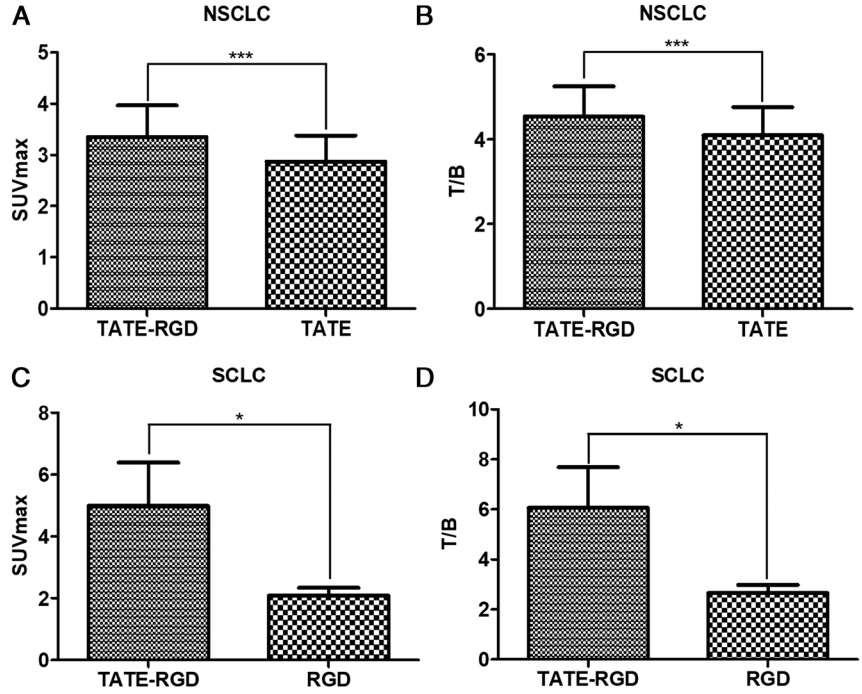

FIGURE 3. Comparison of the SUVmax (**A** and **C**) and the T/B ratios (**B** and **D**) of ^{68}Ga-NOTA-3P-TATE-RGD (TATE-RGD) uptake and ^{68}Ga-NOTA-TATE (TATE) uptake in NSCLC (upper row), as well as TATE-RGD uptake and ^{68}Ga-NOTA-RGD (RGD) uptake in SCLC (lower row). In NSCLC, TATE-RGD uptake was significantly higher than TATE uptake (***P < 0.001). In SCLC, TATE-RGD uptake was significantly higher than RGD uptake (*P < 0.05).

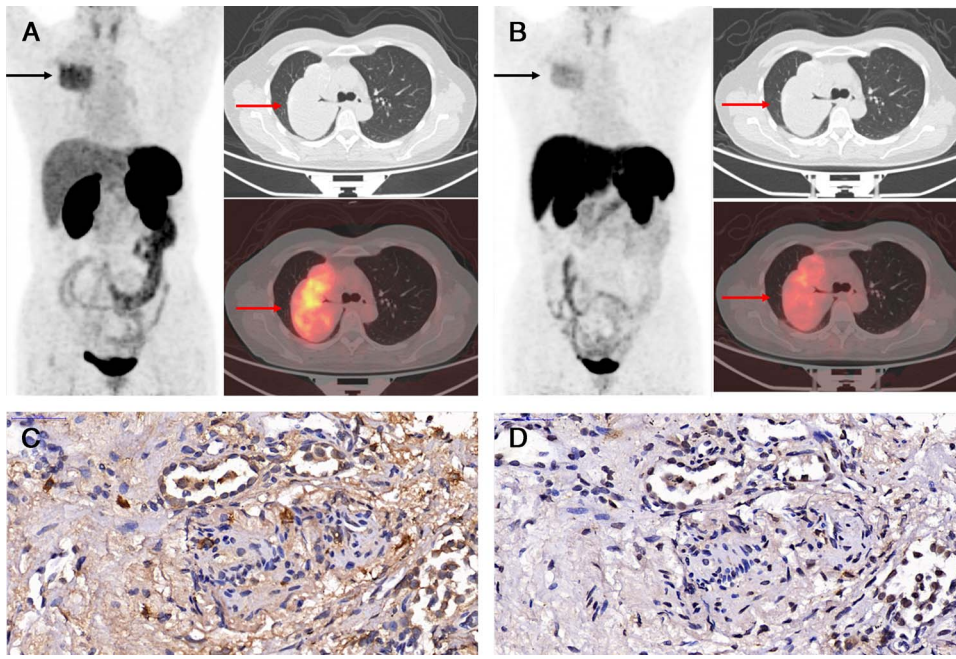

FIGURE 4. Comparison of ^{68}Ga-NOTA-3P-TATE-RGD PET/CT and ^{68}Ga-NOTA-TATE PET/CT in a 57-year-old woman with right lung adenocarcinoma. Maximum intensity projection, CT, and transaxial PET/CT fusion images of ^{68}Ga-NOTA-3P-TATE-RGD PET/CT (**A**) and ^{68}Ga-NOTA-TATE PET/CT (**B**) demonstrated the difference in the uptake of the two tracers in the same tumor of the same patient. The SUVmax of the primary lung tumor was 3.87 and 3.32, respectively. Immumohistochemical staining showed strong staining for integrin $\alpha_v\beta_3$ (**C**) and moderate staining for SSTR2A (**D**).

strong positivity, and integrin $\alpha_v\beta_3$ staining was negative or mildly positive (Fig. 5).

Among the 12 patients with NEN, 8 were diagnosed as NET. The SUVmax of ^{68}Ga-NOTA-3P-TATE-RGD were 24.12 ± 22.39, significantly higher than those of ^{18}F-FDG (3.75 ± 2.81, n = 8, P = 0.0241); the T/B ratios of ^{68}Ga-NOTA-3P-TATE-RGD were 36.13 ± 33.84, also significantly higher than those of ^{18}F-FDG (2.91 ± 1.71, n = 8, P = 0.0234) (Figs. 6 and 7). In the other 4 cases

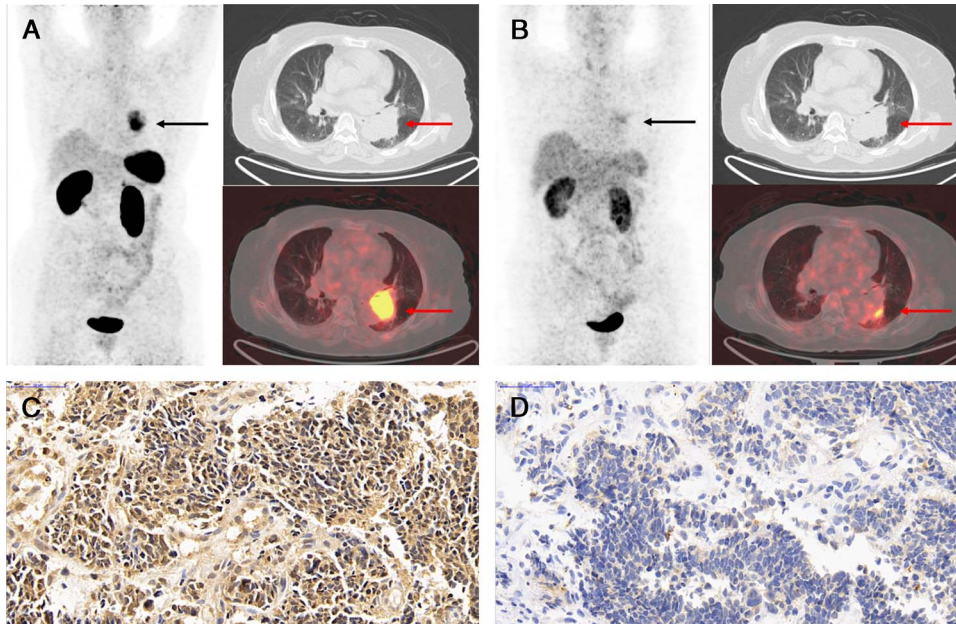

FIGURE 5. Comparison of ^{68}Ga-NOTA-3P-TATE-RGD PET/CT and ^{68}Ga-NOTA-RGD PET/CT in a 60-year-old woman with a small-cell lung cancer. Maximum intensity projection, CT, and transaxial PET/CT fusion images showed intense uptake of ^{68}Ga-NOTA-3P-TATE-RGD (**A**, SUVmax, 18.21 and mild to moderate uptake of ^{68}Ga-NOTA-RGD (SUVmax, 4.72) in the primary tumor at the left hilar region (**B**). Immumohistochemical staining showed strong staining for SSTR2A (**C**) but mild staining for integrin $\alpha_v\beta_3$ (**D**).

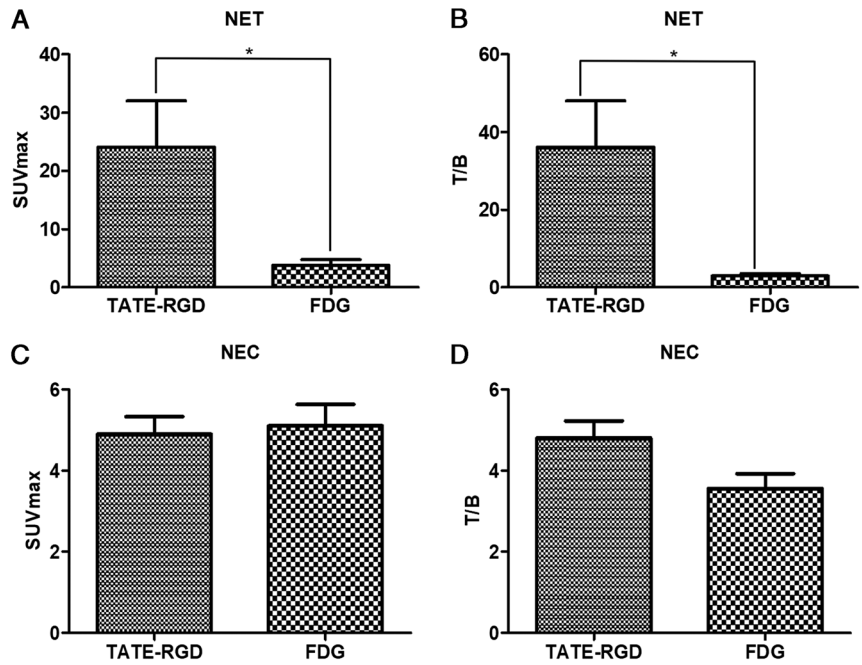

FIGURE 6. Comparison of the SUVmax (**A** and **C**) and the T/B ratios (**B** and **D**) of ^{68}Ga-NOTA-3P-TATE-RGD (TATE-RGD) uptake and ^{18}F-FDG (FDG) uptake in NET (upper row) and NEC (lower row). In NET, TATE-RGD uptake was significantly higher than FDG uptake (*$P < 0.05$). In NEC, there were no significant difference between TATE-RGD uptake and RGD uptake ($P = 0.8282$ for SUVmax; $P = 0.1833$ for T/B ratio).

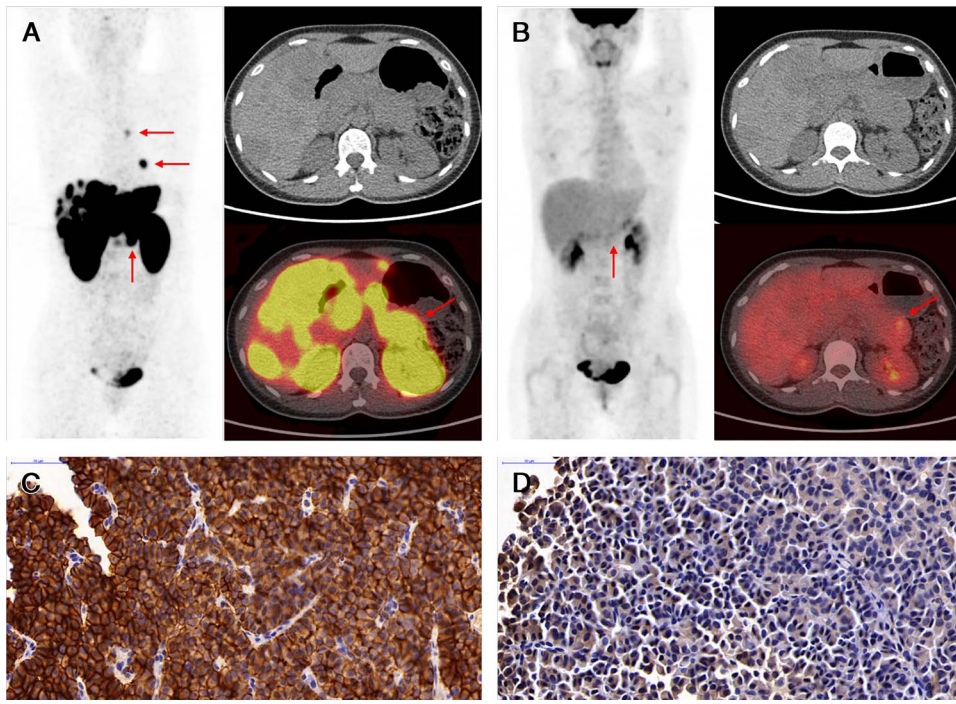

FIGURE 7. Comparison of ^{68}Ga-NOTA-3P-TATE-RGD PET/CT and ^{18}F-FDG PET/CT in a 45-year-old woman with pancreatic NET G2 (Ki-67 index 8%) with multiple liver metastases and lymph node metastases. Maximum intensity projection, CT, and transaxial PET/CT fusion images showed intense uptake of ^{68}Ga-NOTA-3P-TATE-RGD (**A**, SUVmax, 20.40) and mild uptake of ^{18}F-FDG (SUVmax, 3.04) in the mass of pancreas tail (**B**). Immumohistochemical staining of liver metastasis biopsy showed strong stains of SSTR2A (**C**) and moderate stains of integrin $\alpha_v\beta_3$ (**D**).

of NEC, the SUVmax of ^{68}Ga-NOTA-3P-TATE-RGD were 4.89 ± 0.87, which had no significant difference with those of ^{18}F-FDG (5.10 ± 1.07, n = 4, P = 0.8282); the T/B ratios of ^{68}Ga-NOTA-3P-TATE-RGD were 4.80 ± 0.85, similar to those ^{18}F-FDG (3.56 ± 0.74, n = 4, P = 0.1833) as well (Figs. 6 and 8). Immunohistochemical staining showed strong positivity of SSTR2A and mild to moderate stains of integrin $\alpha_v\beta_3$ in the NET (Fig. 7) and mild to moderate expression of SSTR2A and moderate to strong stains of integrin $\alpha_v\beta_3$ in the NEC (Fig. 8).

DISCUSSION

Multimeric peptide-based radiotracers had shown advantages in many studies.[9,10,17–26] Homomultimers had a polyvalency effect that may enhance the affinity and tumor uptake of the peptide radiotracers.[9,10,17–19] Some researchers also synthesized heterodimeric peptides that contained motifs recognizing 2 different receptors.[20–26] Heterodimers hold a promise to bind any of the 2 receptors, which may result in higher sensitivity by providing more chances to bind effective receptors. The radiolabeled heterodimers exhibited dual receptor targeting properties both in vitro and in vivo. Heterodimers with complementary motifs might be promising agents with higher sensitivity over the corresponding monomers in the detection of tumors with expression of each single receptor and double receptors.

^{68}Ga-labeled TATE is an excellent tracer for the evaluation SCLC, which is characterized by high SSTR2 expression, especially the SSTR2A expression.[7] The use of radiolabeled somatostatin analogs for the diagnosis and treatment of SCLC has also been proved useful.[27,28] However, in the evaluation of lung tumors, the uptake ^{68}Ga-labeled TATE in NSCLC seemed to be relatively low because of the light to moderate SSTR2 expression.[29] On the other hand, integrin $\alpha_v\beta_3$ staining was generally increased in NSCLC. RGD-based tracers targeting integrin $\alpha_v\beta_3$ have already been used in the diagnosis and staging of NSCLC using PET/CT.[15,16] The diagnostic value of ^{68}Ga-NOTA-PRGD2 for lung cancer was almost comparable to that of ^{18}F-FDG PET/CT. Moreover, ^{68}Ga-NOTA-PRGD2 PET/CT is more specific than ^{18}F-FDG PET/CT in assessing lymph node metastasis.[15] However, the uptake of ^{68}Ga-RGD2 in SCLC is significantly lower than that in NSCLC because of the lower integrin $\alpha_v\beta_3$ expression in SCLC.[16] In this study, we found that the ^{68}Ga-NOTA-3P-TATE-RGD uptake in NSCLC, contributed by both TATE motif and RGD motif, was significantly higher than the ^{68}Ga-NOTA-TATE uptake. We also confirmed that SCLC tumor showed only mild uptake of ^{68}Ga-NOTA-RGD, and the integrin $\alpha_v\beta_3$ staining was only slightly positive. However, owing to the intense SSTR2A expression in SCLC, the ^{68}Ga-NOTA-3P-TATE-RGD uptake was significantly higher than the ^{68}Ga-NOTA-RGD uptake. Therefore, the novel heterodimer radiotracer ^{68}Ga-NOTA-3P-TATE-RGD complements the advantage of each single target tracer in the evaluation of lung cancer and overcomes the deficiency of ^{68}Ga-labeled TATE in the evaluation of NSCLC and ^{68}Ga-labeled RGD in the evaluation of SCLC.

Similarly, ^{18}F-FDG is the most common tracer used in evaluation of various kinds of tumor, but it showed limitation in evaluation of NET, even if the tumor had multiple metastases. ^{68}Ga-labeled TATE held advantages in the evaluation of NEN. However, it is insufficient for the evaluation of NEC. Therefore, some NEN patients had to undergo both ^{68}Ga-labeled TATE PET/CT and ^{18}F-FDG PET/CT for a full evaluation. In this study, we found that the ^{68}Ga-NOTA-3P-TATE-RGD imaging not only might overcome the deficiency of ^{68}Ga-labeled TATE imaging in the evaluation of NEC through the added binding of RGD motif but also showed broad tumor detection ability that may overcome the limitation of

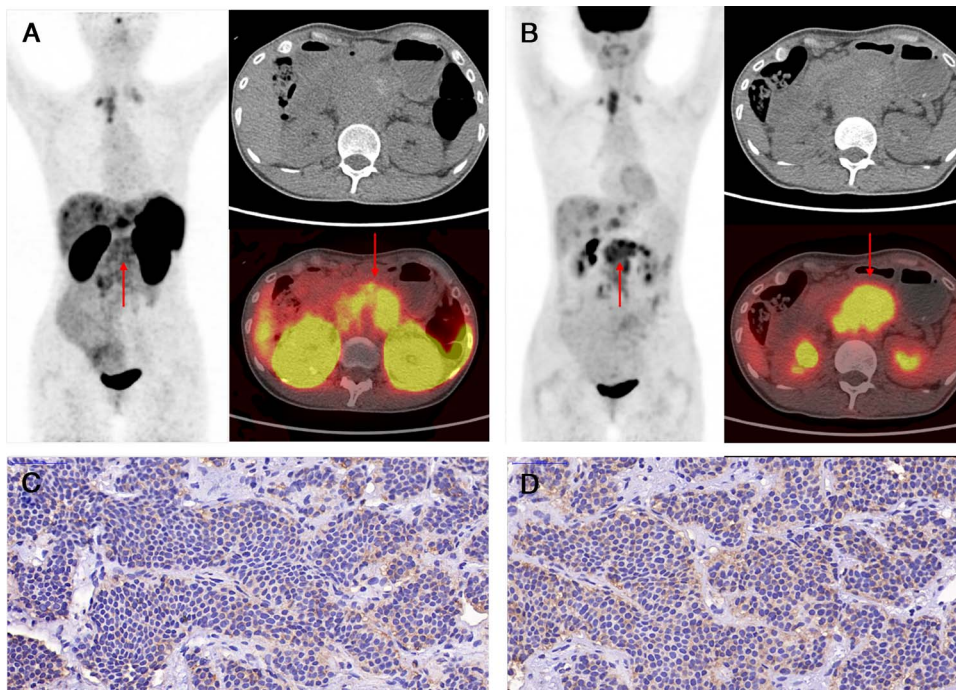

FIGURE 8. Comparison of ^{68}Ga-NOTA-3P-TATE-RGD PET/CT and ^{18}F-FDG PET/CT in a 39-year-old woman with pancreatic NEC (Ki-67 index 60%) with multiple liver metastases and lymph node metastases. Maximum intensity projection, CT, and transaxial PET/CT fusion images showed intense uptake of ^{68}Ga-NOTA-3P-TATE-RGD (**A**, SUVmax, 5.58) and ^{18}F-FDG (**B**, SUVmax, 5.97) in the mass of pancreas. Immumohistochemical staining showed mild to moderate stains of SSTR2A (**C**) and moderate stains of integrin $\alpha_v\beta_3$ (**D**).

^{18}F-FDG PET/CT in the evaluation of NET. However, this is only a pilot proof-of-concept study. Further investigations are needed to confirm the full value of this novel PET tracer. For example, as an imaging method targeting both SSTR2 and integrin αvβ3, ^{68}Ga-NOTA-3P-TATE-RGD PET/CT might be used for response evaluation of a broad range of tumors with overexpression of any of the receptors.

In this first-in-human study, only a trace amount (30–50 μg) of compound NOTA-3P-TATE-RGD was used for labeling; therefore, no biologic or adverse effect was observed in all patients who were administered the ^{68}Ga-NOTA-3P-TATE-RGD injection. The image quality of the ^{68}Ga-NOTA-3P-TATE-RGD PET/CT images was good with a low background uptake, especially for lung cancer detection and lymph node metastasis evaluation. Thus, all known primary tumors of NSCLC and SCLC were observed with high contrast. However, the tracers in kidneys were intense, which may be a defect if considering using ^{177}Lu- or ^{90}Y-labeled TATE-RGD for peptide receptor radionuclide therapy (PRRT). In that case, further modification of the tracer may be needed to reduce the kidney uptake. The spleen also showed intense ^{68}Ga-NOTA-3P-TATE-RGD uptake (SUVmean = 13.02 ± 2.90) but lower than the uptake of ^{68}Ga-NOTA-TATE. The liver uptake of ^{68}Ga-NOTA-3P-TATE-RGD (SUVmean = 1.94 ± 0.40) was mild, significantly lower than that of ^{68}Ga-NOTA-TATE but mildly higher than that of ^{68}Ga-NOTA-RGD.

There are some limitations of this study. First, with intense uptake of ^{68}Ga-NOTA-3P-TATE-RGD in the kidneys, we did not coinfuse cationic amino acids to inhibit the renal tubular reabsorption. Second, in ethical consideration, the patients enrolled to undergo ^{68}Ga-NOTA-3P-TATE-RGD PET/CT was compared with only one other scan, specifically with ^{68}Ga-NOTA-TATE PET/CT in evaluation of NSCLC, with ^{68}Ga-NOTA-RGD PET/CT in SCLC and with ^{18}F-FDG PET/CT in NEN, barely to demonstrate the complementary values of the new tracer over the limitation of the single-target tracers and ^{18}F-FDG. Third, the patient number enrolled in this study was still small. Nonetheless, this preliminary study merits further clinical investigation with more patients.

CONCLUSIONS

This first-in-human, proof-of-concept study has demonstrated the safety and efficacy of ^{68}Ga-NOTA-3P-TATE-RGD, a novel heterodimeric PET tracer designed to target both SSTR2 and integrin $\alpha_v\beta_3$ receptors. The dual-targeting agent not only makes up for the deficiency of each single target agents in the evaluation of lung cancer subtypes but also shows increased sensitivity over ^{18}F-FDG in the detection of NENs. Further studies are needed to prove its values in detection of a wider range of tumors with a single scan.

REFERENCES

1. Wu H, Huang J. PEGylated peptide-based imaging agents for targeted molecular imaging. *Curr Protein Pept Sci*. 2016;17:582–595.
2. Dong C, Liu Z, Wang F. Peptide-based radiopharmaceuticals for targeted tumor therapy. *Curr Med Chem*. 2014;21:139–152.
3. Dijkgraaf I, Boerman OC, Oyen WJ, et al. Development and application of peptide-based radiopharmaceuticals. *Anticancer Agents Med Chem*. 2007; 7:543–551.
4. Cuccurullo V, Prisco MR, Di Stasio GD, et al. Nuclear medicine in patients with NET: radiolabeled somatostatin analogues and their brothers. *Curr Radiopharm*. 2017;10:74–84.
5. Sundin A. Radiological and nuclear medicine imaging of gastroenteropancreatic neuroendocrine tumors. *Best Pract Res Clin Gastroenterol*. 2012;26:803–818.
6. Righi L, Volante M, Tavaglione V, et al. Somatostatin receptor tissue distribution in lung neuroendocrine tumors: a clinicopathologic and immunohistochemical study of 218 'clinically aggressive' cases. *Ann Oncol*. 2010;21: 548–555.
7. Papotti M, Croce S, Bellò M, et al. Expression of somatostatin receptor types 2, 3 and 5 in biopsies and surgical specimens of human lung tumor: correlation with preoperative octreotide scintigraphy. *Virchows Arch*. 2001;439: 787–797.
8. Walker R, Deppen S, Smith G, et al. ^{68}Ga-DOTATATE PET/CT imaging of indeterminate pulmonary nodules and lung cancer. *PLOS One*. 2017;12:e0171301.
9. Li ZB, Chen K, Chen X. ^{68}Ga-labeled multimeric RGD peptides for microPET imaging of integrin αvβ3 expression. *Eur J Nucl Med Mol Imaging*. 2008;35: 1100–1108.
10. Wu Z, Li ZB, Cai W, et al. ^{18}F-labeled mini-PEG spacered RGD dimer (^{18}F-FPRGD2): synthesis and micro-PET imaging of αvβ3 integrin expression. *Eur J Nucl Med Mol Imaging*. 2007;34:1823–1831.
11. Ji S, Zheng Y, Shao G, et al. Integrin $\alpha_v\beta_3$-targeted radiotracer ^{99m}Tc-3P-RGD$_2$ useful for noninvasive monitoring of breast tumor response to antiangiogenic linifanib therapy but not anti-integrin $\alpha_v\beta_3$ RGD$_2$ therapy. *Theranostics*. 2013;3:816–830.
12. Li D, Zhao X, Zhang L, et al. ^{68}Ga-PRGD2 PET/CT in the evaluation of glioma: a prospective study. *Mol Pharm*. 2014;11:3923–3929.
13. Beer AJ, Grosu AL, Carlsen J, et al. [^{18}F]galacto-RGD positron emission tomography for imaging of αvβ3 expression on the neovasculature in patients with squamous cell carcinoma of the head and neck. *Clin Cancer Res*. 2007; 13:6610–6666.
14. Kenny LM, Coombes RC, Oulie I, et al. Phase I trial of the positron-emitting Arg-Gly-Asp (RGD) peptide radioligand ^{18}F-AH111585 in breast cancer patients. *J Nucl Med*. 2008;49:879–886.
15. Zheng K, Liang N, Zhang J, et al. ^{68}Ga-NOTA-PRGD2 PET/CT for integrin imaging in patients with lung cancer. *J Nucl Med*. 2015;56:1823–1827.
16. Kang F, Wang Z, Li G, et al. Inter-heterogeneity and intra-heterogeneity of αvβ3 in non-small cell lung cancer and small cell lung cancer patients as revealed by ^{68}Ga-RGD2 PET imaging. *Eur J Nucl Med Mol Imaging*. 2017;44: 1520–1528.
17. Liu S. Radiolabeled multimeric cyclic RGD peptides as integrin αvβ3 targeted radiotracers for tumor imaging. *Mol Pharm*. 2006;3:472–487.
18. Liu S, Hsieh WY, Jiang Y, et al. Evaluation of a ^{99m}Tc-labeled cyclic RGD tetramer for noninvasive imaging integrin αvβ3-positive breast cancer. *Bioconjug Chem*. 2007;18:438–446.
19. Li ZB, Cai W, Cao Q, et al. ^{64}Cu-labeled tetrameric and octameric RGD peptides for small-animal PET of tumor αvβ3 integrin expression. *J Nucl Med*. 2007;48:1162–1171.
20. Liu Z, Niu G, Wang F, et al. ^{68}Ga-labeled NOTA-RGD-BBN peptide for dual integrin and GRPR-targeted tumor imaging. *Eur J Nucl Med Mol Imaging*. 2009;36:1483–1494.
21. Liu Z, Yan Y, Liu S, et al. ^{18}F, ^{64}Cu, and ^{68}Ga labeled RGD-bombesin heterodimeric peptides for PET imaging of breast cancer. *Bioconjug Chem*. 2009; 20:1016–1025.
22. Zhang J, Niu G, Lang L, et al. Clinical translation of a dual integrin αvβ3- and gastrin-releasing peptide receptor-targeting PET radiotracer, ^{68}Ga-BBN-RGD. *J Nucl Med*. 2017;58:228–234.
23. Zhang J, Mao F, Niu G, et al. ^{68}Ga-BBN-RGD PET/CT for GRPR and integrin $\alpha_v\beta_3$ imaging in patients with breast cancer. *Theranostics*. 2018;8:1121–1130.
24. Shallal HM, Minn I, Banerjee SR, et al. Heterobivalent agents targeting PSMA and integrin-αvβ3. *Bioconjug Chem*. 2014;25:393–405.
25. Eder M, Schafer M, Bauder-Wust U, et al. Preclinical evaluation of a bispecific low-molecular heterodimer targeting both PSMA and GRPR for improved PET imaging and therapy of prostate cancer. *Prostate*. 2014;74:659–668.
26. Luo H, England CG, Shi S, et al. Dual targeting of tissue factor and CD105 for preclinical PET imaging of pancreatic cancer. *Clin Cancer Res*. 2016;22: 3821–3830.
27. Schmitt A, Bernhardt P, Nilsson O, et al. Differences in biodistribution between ^{99m}Tc-depreotide, ^{111}In-DTPA-octreotide, and ^{177}Lu-DOTA-Tyr3-octreotate in a small cell lung cancer animal model. *Cancer Biother Radiopharm*. 2005; 20:231–236.
28. Sollini M, Farioli D, Froio A, et al. Brief report on the use of radiolabeled somatostatin analogs for the diagnosis and treatment of metastatic small-cell lung cancer patients. *J Thorac Oncol*. 2013;8:1095–1101.
29. Dimitrakopoulou-Strauss A, Georgoulias V, Eisenhut M, et al. Quantitative assessment of SSTR2 expression in patients with non-small cell lung cancer using ^{68}Ga-DOTATOC PET and comparison with ^{18}F-FDG PET. *Eur J Nucl Med Mol Imaging*. 2006;33:823–830.